Discrete Surface Ricci Flow: Theory and Applications

Miao Jin, Junho Kim, and Xianfeng David Gu

State University of New York at Stony Brook,
Stony Brook, NY USA
gu@cs.sunysb.edu
http://www.cs.sunysb.edu/~gu

Abstract. Conformal geometry is in the core of pure mathematics. Conformal structure is more flexible than Riemaniann metric but more rigid than topology. Conformal geometric methods have played important roles in engineering fields. This work introduces a theoretically rigorous and practically efficient method for computing Riemannian metrics with prescribed Gaussian curvatures on discrete surfaces - discrete surface Ricci flow, whose continuous counter part has been used in the proof of Poincaré conjecture. Continuous Ricci flow conformally deforms a Riemannian metric on a smooth surface such that the Gaussian curvature evolves like a heat diffusion process. Eventually, the Gaussian curvature becomes constant and the limiting Riemannian metric is conformal to the original one.

In the discrete case, surfaces are represented as piecewise linear triangle meshes. Since the Riemannian metric and the Gaussian curvature are discretized as the edge lengths and the angle deficits, the discrete Ricci flow can be defined as the deformation of edge lengths driven by the discrete curvature. The existence and uniqueness of the solution and the convergence of the flow process are theoretically proven, and numerical algorithms to compute Riemannian metrics with prescribed Gaussian curvatures using discrete Ricci flow are also designed.

Discrete Ricci flow has broad applications in graphics, geometric modeling, and medical imaging, such as surface parameterization, surface matching, manifold splines, and construction of geometric structures on general surfaces.

Key words: Conformal geometry, Discrete Ricci flow, Riemannian metric, uniformization, global conformal parametrization, manifold

1 Introduction

Conformal geometry offers rigorous and powerful theoretic tools for practical engineering applications. Ricci flow is a novel curvature flow method in computational conformal geometry, which will play important roles in practice because of its universality and flexibility.

1.1 Conformal geometry

Conformal geometry is in the core of pure mathematics, which is the intersection of complex analysis, algebraic topology, differential geometry, algebraic geometry, and many other fields in mathematics.

Conformal geometry studies the conformal structures of Riemann surfaces. Conformal structure is a fundamental geometric structure, which is more rigid than topological structure but more flexible than Riemannian metric structure. All surfaces can be deformed to three canonical spaces preserving geometric information. This fact greatly simplifies the theoretic arguments in mathematics. Furthermore, all surfaces can be classified according to their conformal structures. The "shape space" of conformal equivalent classes form a finite dimensional Riemannian manifold, which offers a universal framework for shape analysis.

With the development of $3D$ acquisition technologies and computational power, conformal geometry plays more and more important roles in engineering fields. For example, conformal geometry has been broadly applied in computer graphics, computer vision, geometric modeling and medical imaging. The theoretic foundation for computational conformal geometry is developing rapidly and many practical algorithms converting classical theories in conformal geometry have been invented.

So far, the computational methodologies in conformal geometry for general surfaces are mainly in the following categories: harmonic maps, holomorphic differentials, and newly invented method in geometric analysis, *Ricci flow*. Ricci flow is very powerful and flexible, which will cause great impact in engineering field. In this work, we mainly focus on the introduction to the theories and algorithms of discrete surface Ricci flow.

1.2   Ricci Flow

Recently, the term of *Ricci flow* becomes popular, due to the fact that it has been applied for the proof of the Poincaré conjecture on 3-manifolds [1–3]. Richard Hamilton introduced the Ricci flow for Riemannian manifolds of any dimension in his seminal work [4] in 1982. Intuitively, a surface Ricci flow is the process to deform the Riemannian metric of the surface. The deformation is proportional to Gaussian curvatures, such that the curvature evolves like the heat diffusion.

It has been considered as a powerful tool for computing the conformal Riemannian metrics with prescribed Gaussian curvatures. For many engineering applications, it is also highly desirable to compute Riemannian metrics on surfaces with prescribed Gaussian curvatures, such as parameterization in graphics, spline construction in geometric modeling, conformal brain mapping in medical images, and so on.

Surface parameterization refers to the process of mapping a surface onto a planar domain. If such a parameterization is known, any functions or signals (e.g., texture) on the flat parametric domain can be easily pulled back to the surface, such that complicated processing on surfaces can be transferred to easy computing on the flat parametric domain. Therefore it is a key ingredient for digital geometry processing, such as texturing [5], deformation [6], and resampling [7]. The process for parameterizing surfaces is quadrivalent to finding a special flat Riemannian metric, with *zero* Gaussian curvatures everywhere.

Constructing splines whose parametric domain is an arbitrarily topological manifold is an important issue for computer-aided geometric modeling [8]. In order to define such parameters and knots of the spline, a special atlas of the surface is required such that all local coordinate transition maps are affine [9]. One way to construct such an atlas is to find a flat metric of the surface first, then locate a collection of patches covering the

whole surface, and flatten each patch using the flat metric to form an atlas. Here again, the key step is to obtain the flat metric of the given surface.

In medical imaging field, it is important to deform the human brain cortex surface to the unit sphere in order to easily compare and register several different brain cortexes on a canonical domain [10]. This is equivalent to find a Riemannian metric on the cortex surface, such that the Gaussian curvature induced by the metric equals to *one* everywhere.

Comparing to existing methods, which can only handle a subproblem in the scope of Euclidean parametrization, Ricci flow can handle arbitrary topologies and find arbitrary conformal mappings, which include not just Euclidean, but also hyperbolic and spherical parameterizations.

The discrete Ricci flow on piecewise linear surfaces was introduced in [11]. The existence and convergence of the discrete Ricci flow for surfaces were established. However, the discrete Ricci flow is not a very efficient algorithm for practical use due to the gradient nature of the flow. Recently, we improve the gradient descent method by the Newton's method and drastically speed up the search for the limiting metric by the order of magnitudes. Furthermore, we generalize the results from constant discrete curvature to arbitrarily prescribed discrete curvature, from the metric induced by the combinatorial structure of the mesh to the induced Euclidean metric. We have developed an effective and complete system to compute Riemannian metrics with prescribed Gaussian curvatures on generally topological surfaces has been developed in this paper based on discrete Euclidean Ricci flow, discrete hyperbolic Ricci flow, and discrete spherical Ricci flow.

1.3   Outline

In the next section 2, we will briefly review most related works in computer graphics field and discrete complex analysis; in Sec. 3, theoretic background in differential geometry and Rieman surface are introduced; in Sec. 4, the theories for major computational methodologies are introduces, including harmonic maps, holomorphic differential forms and Ricci flow; in Sec.5, the algorithm and theories of discrete Ricci flow are thoroughly explained; practical applications are given in Sec.6; in the conclusion Sec.7, future directions are pointed out.

2   Previous Work

In computer graphics and discrete mathematics, much sound research has focused on discrete conformal parameterizations. Here, we briefly overview related work, and refer readers to [12, 13] for thorough surveys.

All parameterizations can be classified according to the type of output produced, which can be *a vector valued function, i.e. a mapping*, *a holomorphic differential form* or *a flat Riemannian metric*. In general, the derivative of a conformal map is a holomorphic 1-form; each holomorphic 1-form induces a flat metric. Therefore, methods which compute metrics are the most general, although they are more expensive to compute.

Mappings First order finite element approximations of the Cauchy-Riemann equations were introduced by Levy et al. [5]. Discrete intrinsic parameterization by minimizing Dirichlet energy was introduced by [14], which is equivalent to least-squares conformal mapping [5]. Discrete harmonic maps were computed using the cotan-formula in [15]. Mean value coordinates were introduced in [16]; these generalize the cotan-formula. All these linear methods can easily incorporate free boundary conditions to improve the quality of the parameterization produced, such as the methods in [14] and [17]. Discrete spherical conformal mappings are used in [18] and [10].

Holomorphic forms Holomorphic forms are used in [19] to compute global conformal surface parameterizations for high genus surfaces. Discrete holomorphy was introduced in [20] using discrete exterior calculus [21]. The problem of computing optimal holomorphic 1-forms to reduce area distortion was considered in [22]. Gortler et al. [23] generalized 1-forms to the discrete case, using them to parameterize genus one meshes. Recently, Tong et al. [24] generalized the 1-form method to incorporate cone singularities.

Metrics There are three major methods for computing edge lengths (or equivalently the angles): angle based flattening, circle packing, and circle patterns.

Sheffer and Sturler [25] introduced the angle based mesh flattening method. This works by posing a constrained quadratic minimization problem seeking to find corner angles which are close to desired angles in a weighted $L2$ norm. The efficiency and stability of ABF are improved in [26] by using advanced numerical algorithm and hierarchical method.

The circle packing method was introduced in [27]. Continuous conformal mappings can be characterized as mapping infinitesimal circles to infinitesimal circles. Circle packings replace infinitesimal circles with finite circles. In the limit of refinement the continuous conformal maps are recovered [28]. Collins and Stephenson [29] have implemented these ideas in their software CirclePack.

The first variational principle for circle packings, was presented in a seminal paper by Colin de Verdière [30]. Circle patterns based on those in Bobenko and Springborn [31] have been applied for parameterization in [32]. Springborn [33] shows that in theory, circle packing and circle patterns are equivalent.

Ricci Flow Recently, a novel curvature flow method in geometric analysis is introduced to prove the Poincaré conjecture, the *Ricci Flow*. Ricci flow refers to conformally deform the Riemannian metric of a surface by its Gaussian curvature, such that the curvature evolves according to a heat diffusion process. Ricci flow is a powerful tool to compute the Riemannian metric by the curvature. It can be applied for discrete conformal parameterizations.

The connection between circle packing and smooth surface Ricci flow [34] was discovered in [11]. Conventional circle packing only considers combinatorics. The discrete Ricci flow method was introduced in [35, 36], which incorporate geometric information and was applied for computing hyperbolic and projective structure and manifold splines.

3 Theoretical Background

In this section, we briefly introduce the major concepts in differential geometry and Riemann surface theory, which are necessary to explain the theory of the Ricci flow. We refer readers to [37, 38] for detailed information.

3.1 Riemannian metric

Suppose $D \subset \mathbb{R}^2$ is a planar domain, a map $\mathbf{r} : D \to \mathbb{R}^3$ is with at least C^2 continuity. Let $\mathbf{r}_i = \frac{\partial \mathbf{r}}{\partial u_i}, i = 1, 2$ be the tangent vectors along the iso-parametric curves, if

$$\mathbf{r}_1 \times \mathbf{r}_2 \neq 0,$$

then $\mathbf{r}$ is called a *regular surface*. The *normal* is defined as

$$\mathbf{n} = \frac{\mathbf{r}_1 \times \mathbf{r}_2}{|\mathbf{r}_1 \times \mathbf{r}_2|},$$

the map $G : \mathbf{r}(u_1, u_2) \to \mathbf{n}(u_1, u_2) \in \mathbb{S}^2$ is called the *Gauss map*, where $\mathbb{S}^2$ is the unit sphere. The length of a general tangent vector $d\mathbf{r} = \mathbf{r}_1 du_1 + \mathbf{r}_2 du_2$ can be computed

$$ds^2 = <d\mathbf{r}, d\mathbf{r}> = (du_1 du_2) \begin{pmatrix} g_{11} & g_{12} \\ g_{21} & g_{22} \end{pmatrix} \begin{pmatrix} du_1 \\ du_2 \end{pmatrix}$$

where $<,>$ is the inner product in $\mathbb{R}^3$, and $g_{ij} = <r_i, r_j>$. The matrix $\mathbf{g} = (g_{ij})$ is called the *Riemannian metric tensor*, which defines the inner products $<,>_\mathbf{g}$ on the tangent planes of the surface. The angles between two tangent vectors can be measured by $\mathbf{g}$. Suppose $\delta\mathbf{r} = \mathbf{r}_1 \delta u_1 + \mathbf{r}_2 \delta u_2$ is another tangent vector, the angle between $d\mathbf{r}$ and $\delta\mathbf{r}$ measured by $\mathbf{g}$ is $\theta_\mathbf{g}$, then

$$\theta_\mathbf{g} = \cos^{-1} \frac{<d\mathbf{r}, \delta\mathbf{r}>_\mathbf{g}}{\sqrt{<d\mathbf{r}, d\mathbf{r}>_\mathbf{g}} \sqrt{<\delta\mathbf{r}, \delta\mathbf{r}>_\mathbf{g}}} \tag{1}$$

Suppose $\lambda : (u_1, u_2) \to \mathbb{R}$ is a real function defined on the surface, then $\bar{\mathbf{g}} = e^{2\lambda(u_1, u_2)} \mathbf{g}$ is another Riemannian metric,

$$<d\mathbf{r}, \delta\mathbf{r}>_{\bar{\mathbf{g}}} = e^{2\lambda} <d\mathbf{r}, \delta\mathbf{r}>_\mathbf{g} \tag{2}$$

The angle between $d\mathbf{r}$ and $\delta\mathbf{r}$ measured by $\bar{\mathbf{g}}$ is $\theta_{\bar{\mathbf{g}}}$, plug Eqn. 2 to 1 directly, we obtain

$$\theta_\mathbf{g} = \theta_{\bar{\mathbf{g}}}.$$

Namely, the angles measured by $\mathbf{g}$ equal to those measured by $\bar{\mathbf{g}}$. Therefore, we say $\bar{\mathbf{g}}$ and $\mathbf{g}$ are *conformally equivalent*. 'conformal' means the angle preserving, while the area distorted, with $e^{2\lambda}$ measuring the area distortion and being called the *conformal factor*.

All Riemannian metrics are surfaces are classified by the conformal equivalence relation, each conformal equivalent class is called a *conformal structure*. Any Riemannian metric on the surface are locally conformal equivalent to the Euclidean flat metric.

Namely, one can choose a special parameters, the change of parameterization doesn't affect the metric, such that the metric is represented as

$$ds^2 = e^{2\lambda}(du_1^2 + du_2^2), \tag{3}$$

such kind of parameterizations are called the *isothermal coordinates* of the surface.

3.2   Gaussian curvature

The Gauss map maps the surface to the unit sphere, the derivative map of the Gauss map is the first order linear approximation to it. The Jacobin of the derivative map measures the local area distortion between the surface and the image on the sphere, which is called the *Gaussian curvature K*. Under the isothermal coordinates Eqn. 3, the Gaussian curvature is represented as

$$K = -e^{-2\lambda}\Delta\lambda,$$

where Δ is the *Laplace operator*,

$$\Delta = \frac{\partial^2}{\partial u_1^2} + \frac{\partial^2}{\partial u_2^2}.$$

$e^{-2\lambda}\Delta$ is called the *Laplace-Beltrami operator*.

Along the boundary of the surface, the tangential component of the curvature of the boundary curve is defined as the *geodesic curvature k*. Under the isothermal coordinates, the geodesic curvature is represented as

$$k = -e^{-\lambda}\partial_{\mathbf{n}}\lambda,$$

where $\mathbf{n}$ is the exterior tangent vector perpendicular to the boundary.

The total curvature of a surface is solely determined by the topology of the surface and independent of the metric. Gauss-Bonnet theorem [37] explains the connection between the total Gaussian curvatures on a surface S and the topology of S.

$$\int_S K dA + \int_{\partial S} k_g ds = 2\pi\chi(S), \tag{4}$$

where $\chi(S)$ is the Euler number of S, $\chi(S) = 2 - 2g - b$, g, b are the genus and the number of the boundaries of the surface.

3.3   Conformal Metric Deformation

Under a conformal metric $\bar{\mathbf{g}}$, the curvatures are changed accordingly, the following *Yamabi equations* describe the relation between the conformal metric deformation and the curvature change, suppose $\bar{\mathbf{g}} = e^{2\lambda}\mathbf{g}$, then

$$\bar{K} = e^{-2\lambda}(K - \Delta\lambda), \bar{k} = e^{-\lambda}(k - \partial_{\mathbf{n}}\lambda), \tag{5}$$
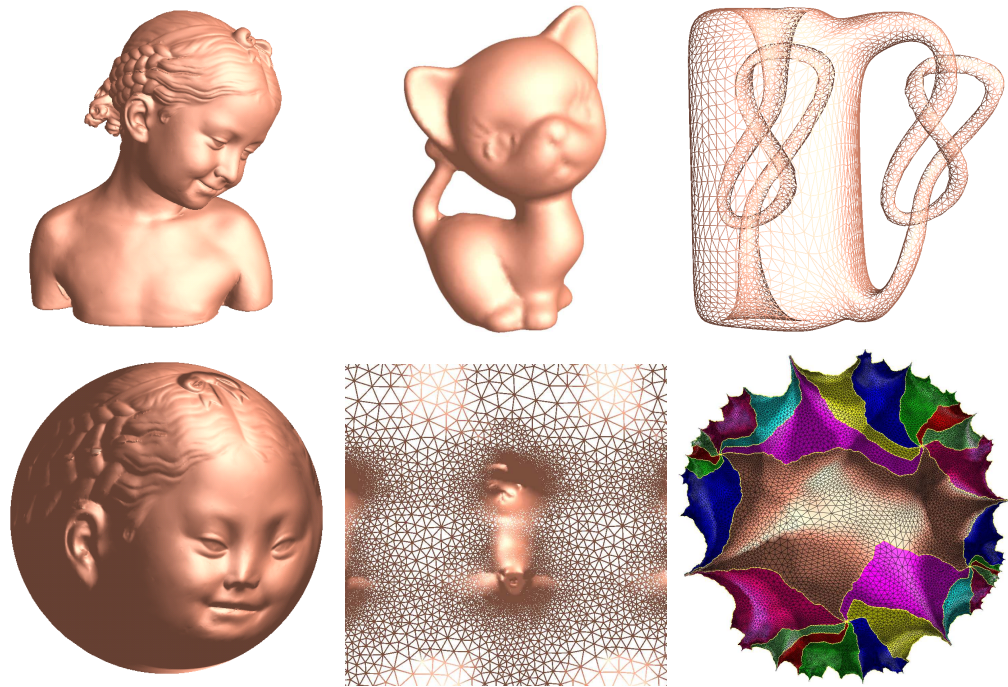
Fig. 1. Uniformization Theorem: all surfaces with Riemannina metric can be conformally embedded onto three canonical spaces: sphere, plane and hyperbolic space.

where Δ is the Laplace-Beltrami operator under the metric $\mathbf{g}$.

It has the fundamental importance to solve the Riemannian metric $\bar{\mathbf{g}}$ from the target curvature $\bar{K}$ and $\bar{k}$. In each conformal equivalent class, there exists a unique metric, such that the induced curvature is one of the three constants everywhere $\{+1, 0, -1\}$. This fact is formulated as the Uniformization theorem [27] .

Theorem 1 (Uniformization Theorem). *Let $(S, \mathbf{g})$ be a compact 2-dimensional Riemannian manifold with Riemannian metric $\mathbf{g}$, then there is a unique metric $\bar{\mathbf{g}}$ conformal to $\mathbf{g}$ with constant Gaussian curvatures. The constant value is one of the $\{+1, 0, -1\}$.*

Such metric is called the *uniformization metric*. According to Gauss-Bonnet theorem (Eqn. 4), the sign of the constant Gaussian curvatures is determined by the Euler number of the surface. Therefore, any closed 2-manifold surface can be locally isometrically embedded onto one of the three canonical surfaces with respect to its Euler number χ; the *sphere* $\mathbb{S}^2$ for genus zero surfaces with $\chi > 0$, the *plane* $\mathbb{E}^2$ for genus one surfaces with $\chi = 0$, and the *hyperbolic space* $\mathbb{H}^2$ for high genus surfaces with $\chi < 0$ (see Fig. 1).

3.4   Universal Covering Space

Suppose S is a surface, then $(\bar{S}, \pi)$ is called the *universal covering* space of S, if $\bar{S}$ is simply connected and locally $\pi : \bar{S} \to S$ is bijective and continuous. Fig. 2(b) shows the universal covering space of the genus one kitten surface (a). A *deck transformation* is an automorphism $\tau : \bar{S} \to \bar{S}$, such that $\pi \circ \tau = \pi$ as shown in Fig. 3. All deck transformations form a group, called the *deck transformation group* and denoted as $Deck(S)$. Suppose $D \subset \bar{S}$ is simply connected, for arbitrary 2 deck transformations τ_1, τ_2, $\tau_1(D) \cap \tau_2(D) = \emptyset$, $\cup_{\tau \in Deck(S)} \tau(D) = \bar{S}$, then D is called a *fundamental domain* of S. The rectangles in Fig.3 illustrate two fundamental domains.

Suppose a point $p \in S$ on the surface, the pre-images of p on the universal covering space are $\pi^{-1}(p) = \{\bar{p}_0, \bar{p}_1, \bar{p}_2, \cdots\} \subset \bar{S}$, then $\pi^{-1}(p)$ has a one to one map to the deck transformation group $Deck(S)$. For any $\bar{p}_k \in \pi^{-1}(p)$, there exists a unique deck transformation $\tau_k \in Deck(S)$, such that $\tau_k(\bar{p}_0) = \bar{p}_k$, see Fig. 3.

The deck transformations of $\bar{S}$ with the uniformization metric are rigid motions in the canonical spaces, which form a group (the *Fuchsian group* in hyperbolic space). Such a group can represent the conformal structure of the surface S.

The universal covering space of a surface with negative Euler number can be embedded isometrically onto the hyperbolic space with the uniformization metric. The common hyperbolic space models include Poincaré disk and Klein model. The Poincaré disk is the unit disk on the complex plane, $|z| < 1$ with the metric $ds^2 = \frac{dzd\bar{z}}{1-\bar{z}z}$. The geodesics are circular arcs perpendicular to the boundary. The Klein model is also the unit disk. The map from the Poincaré model to the Klein model is

$$\beta(z) = \frac{2z}{1 + z\bar{z}}.$$

3.5   Riemann Surface

A Riemann surface is a surface with a complex structure, such that complex analysis can be defined on the surface.
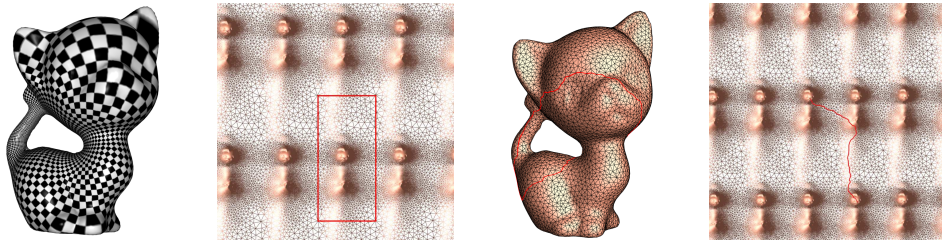

Fig. 2. (a) The kitten surface with the flat metric computed using Ricci flow method. (b) Its universal covering space and one fundamental domain (the rectangle). (c) A loop on surface. (d) The loop lifted to a path in UCS
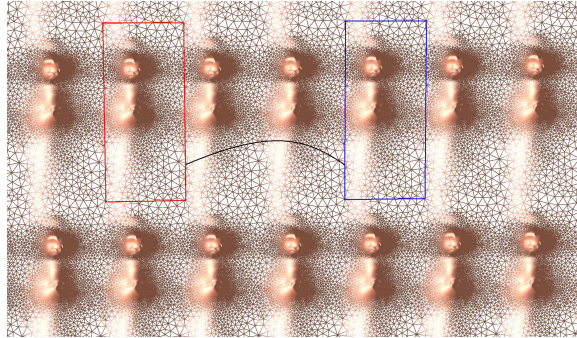
Fig. 3. The universal covering space of the bunny surface, a deck transformation maps the left foundamental domain to the right.

Suppose $f : \mathbb{C} \to \mathbb{C}$ is a complex function $f(x, y) = (u(x, y), v(x, y))$, f is *holomorphic*, if it satisfies the following *Cauchy-Riemann equations*,

$$\frac{\partial u}{\partial x} = \frac{\partial v}{\partial y}, \frac{\partial u}{\partial y} = -\frac{\partial v}{\partial x}.$$

If a holomorphic function f is bijection, and the inverse f^{-1} is also holomorphic, then f is *biholomorphic*.
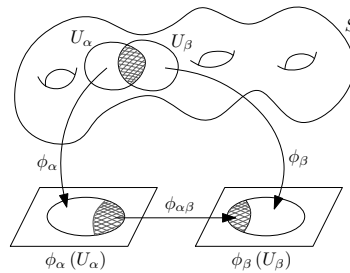

Fig. 4. A surface is covered by an atlas. If all chart transitions are holomorphic, the atlas is a conformal atlas. If all local coordinates are isothermal, the surface is a Riemann surface.

As shown in Fig.4, suppose S is a surface covered by a collection of open sets $\{U_\alpha\}$, $S \subset \bigcup_\alpha U_\alpha$. A chart is (U_α, ϕ_α), where $\phi_\alpha : U_\alpha \to \mathbb{R}^2$ is a homeomorphism, and the chart transition function $\phi_{\alpha\beta} : \phi_\alpha(U_\alpha \cap U_\beta) \to \phi_\beta(U_\alpha \cap U_\beta)$, $\phi_{\alpha\beta} = \phi_\beta \circ \phi_\alpha^{-1}$. The collection of the charts $\mathscr{A} = \{(U_\alpha, \phi_\alpha)\}$ is called the atlas of S. If all chart transition functions are biholomorphic, then the atlas is called a *conformal structure* of the surface.

Suppose S has a Riemannian metric **g**, and all the local coordinates of the conformal structure are isothermal, then S is called a *Riemann surface*.

Suppose ω is a complex differential form, such that on each chart (U_α, ϕ_α) with local complex parameter z_α, $\omega = f_\alpha(z_\alpha)dz_\alpha$. Suppose two charts overlap $U_\alpha \cap U_\beta$, then

$$f_\beta(z_\beta) = f_\alpha(z_\alpha(z_\beta))\frac{dz_\alpha}{dz_\beta}.$$

Suppose $(S_1, \mathscr{A}_1)$ and $(S_2, \mathscr{A}_2)$ are two Riemann surfaces, $\mathscr{A}_i$'s are their conformal structures. Suppose (U_α, ϕ_α) is a local chart of $\mathscr{A}_1$, (V_β, ψ_β) is a local chart of $\mathscr{A}_2$. $\phi : S_1 \to S_2$ is a *conformal map* if and only if

$$\psi_\beta \circ \phi \circ \phi_\alpha^{-1} : \phi_\alpha(U_\alpha) \to \psi_\beta(V_\beta)$$

is biholomorphic. A conformal map preserves angles.

4 Computational Methodology

In this section, we briefly introduce the theoretic aspects of different computational methodologies. These methods inspire the discrete computational algorithms.

4.1 Harmonic Maps

Suppose $\phi : S \to \mathbb{R}$ is a real function on the surface S, which has a metric $\mathbf{g}$, the *harmonic energy* of ϕ is defined as

$$E(\phi) = \int_S |\nabla_{\mathbf{g}}\phi|^2 dA_{\mathbf{g}}, \tag{6}$$

where $\nabla_{\mathbf{g}}$ and $dA_{\mathbf{g}}$ are the gradient operator and the area element under the metric $\mathbf{g}$, respectively. If (u_1, u_2) are isothermal coordinates with $e^{-2\lambda}$ as the conformal factor, then

$$\nabla_{\mathbf{g}} = e^{-\lambda}(\frac{\partial}{\partial u_1} \ \frac{\partial}{\partial u_2})^T, dA_{\mathbf{g}} = e^{2\lambda} du_1 du_2.$$

A *harmonic function* is a critical point of the harmonic energy. A harmonic function satisfies the following Laplace equation,

$$\Delta_{\mathbf{g}}\phi = 0, \Delta_{\mathbf{g}} = e^{-2\lambda}(\frac{\partial^2}{\partial u_1^2} + \frac{\partial^2}{\partial u_2^2}),$$

where $\Delta_{\mathbf{g}}$ is called the *Laplace-Beltrami operator* determined by the metric $\mathbf{g}$. A harmonic map satisfies the *mean-value* property, for any point p

$$\phi(p) = \int_D \phi(q)dA,$$

where D is a small disk centered at point p.

Suppose ϕ is a map $\phi : S \to \mathbb{R}^n$, then ϕ is a harmonic map, if all its components are harmonic functions. All conformal maps must be harmonic, but the inverse is not true, except genus 0 closed surface, whose harmonic map is also conformal.

Fig. 5 illustrates a conformal parameterization result using harmonic map method.

Fig. 5. Conformal parameterization using harmonic map.

The common way to compute a harmonic map is to construct a map first, then use the following heat flow method to diffuse the map to be harmonic:

$$\frac{d\phi}{dt} = -\Delta_{\mathbf{g}}\phi, \qquad (7)$$

the heat flow is with specific constraints. For example, in order to compute the conformal map from a genus zero closed surface to the unit sphere, the nonlinear heat flow method is applied in [10].

4.2   Holomorphic 1-forms

Definition 1 (Holomorphic 1-forms). *Suppose ω is a complex differential form, such that on each chart (U_α, ϕ_α) with local complex parameter z_α, $\omega = f_\alpha(z_\alpha)dz_\alpha$. Suppose two charts overlap $U_\alpha \cap U_\beta$, then*

$$f_\beta(z_\beta) = f_\alpha(z_\alpha(z_\beta))\frac{dz_\alpha}{dz_\beta}.$$

A holomorphic 1-form $f(z)dz$ on a Riemann surface, defines a field of line elements dz, by the requirement that $f(z)dz$ is real, namely $\arg f(z) = -\arg dz (mod\,\pi)$. The integral curves of this field of line elements are called a *horizontal trajectories*. If $f(z)dz$ is imaginary, then the integral curves of the field of line elements are called a *vertical trajectories*.

Figure 6 illustrates the trajectories on surfaces. On the bunny surface, the horizontal and the vertical trajectories are explicitly illustrated. On the David head surface and the David body surface, the conformal grids formed by the trajectories are illustrated using checker board texture mapping.

According to Poincaré-Hopf theorem, each holomorphic 1-form has zero points, where $f(z_\alpha) = 0$. In general, the total number of zero points equals to the Euler number $|\chi(S)|$. Locally, one can construct a conformal chart in a neighborhood of a zero point, such that the 1-form is $z_\alpha dz_\alpha$. Fig.7 shows the two zero points of a holomorphic 1-form on a genus two surface.
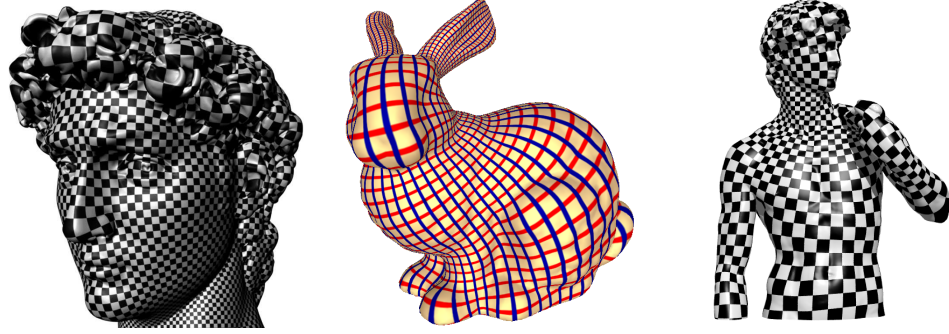
Fig. 6. Holomorphic forms on surfaces. The horizontal and vertical trajectories of the holomorphic forms are illustrated on the bunny surface. The conformal grids formed by the horizontal and vertical trajectories are demonstrated by the checker board texture mapping on the David head surface and the David body model.

The computational algorithm for holomorphic 1-forms is as the following: first a cohomology group basis is constructed using algebraic topological methods, then cohomology basis are diffused to be harmonic forms using the heat flow method in Eqn.9, finally the conjugate of harmonic forms are computed to form the holomorphic 1-forms. Details can be found in [19].

4.3 Ricci Flow

Suppose S is a smooth surface with a Riemannian metric **g**. The Ricci flow is the process to deform the metric **g**(t) by its induced Gaussian curvature $K(t)$, where t is the time parameter, such that the curvature evolves according to a heat diffusion,

$$\frac{dg_{ij}(t)}{dt} = -2K(t)g_{ij}(t). \tag{8}$$

Suppose $T(u_1, u_2, t)$ is a temperature field on the surface, then according to the thermal dynamics, the temperature field will evolve governed by the following heat diffusion equation,

$$\frac{T(t)}{dt} = -\Delta_{\mathbf{g}}T(t).$$

In Ricci flow, the curvature evolution is exactly the same as heat diffusion on the surface, as follows:

$$\frac{K(t)}{dt} = -\Delta_{\mathbf{g}(t)}K(t), \tag{9}$$

where $\Delta_{\mathbf{g}(t)}$ is the Laplace-Beltrami operator induced by the metric **g**(t). We can simplify the Ricci flow equation 8. Let $g(t) = e^{2\lambda(t)}g(0)$, then Ricci flow is

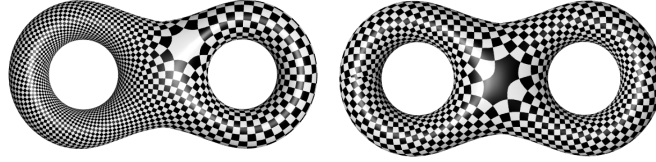$$\frac{d\lambda(t)}{dt} = -2K(t). \tag{10}$$

Fig. 7. The octagons in the centers are zero points of a holomorphic 1-form on a genus two surface.

The following theorems postulate that the Ricci flow defined in Eqn. 8 is convergent and lead to conformal uniformization metric.

Theorem 2 (Hamilton 1982 [34]). *For a closed surface of non-positive Euler characteristic, if the total area of the surface is preserved during the flow, the Ricci flow will converge to a metric such that the Gaussian curvature is constant everywhere.*

Theorem 3 (Chow 1991 [39]). *For a closed surface of positive Euler characteristic, if the total area of the surface is preserved during the flow, the Ricci flow will converge to a metric such that the Gaussian curvature is constant everywhere.*

The corresponding metric $\mathbf{g}(\infty)$ is the *uniformization metric*. Moreover, at any time t, the metric $\mathbf{g}(t)$ is conformal to the original metric $\mathbf{g}(0)$.

The Ricci flow can be easily modified to compute a metric with a *prescribed* curvature $\bar{K}$, and then the flow becomes

$$\frac{dg_{ij}(t)}{dt} = 2(\bar{K} - K)g_{ij}(t). \tag{11}$$

With this modification, any target curvatures $\bar{\mathbf{K}}$, which are admissible with the Gauss-Bonnet theorem, can be induced from the solution metric $\mathbf{g}(\infty)$.

5   Discrete Ricci Flow

In engineering fields, smooth surfaces are often approximated by simplicial complexes (triangle meshes). We consider a triangle mesh Σ with vertex set V, edge set E and face set F.

We say Σ is with Euclidean background geometry, or simply Σ is an *Euclidean mesh*, if each of its faces is realizable on the Euclidean plane. Similarly, we can define meshes with spherical or hyperbolic background geometries respectively.
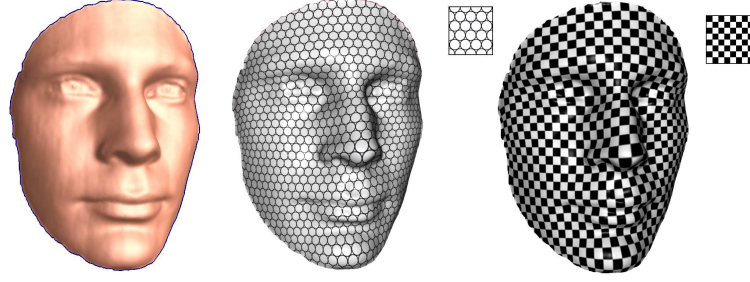
Fig. 8. Conformal parameterizations map infinitesimal circles to infinitesimal circles and preserve the intersection angles among the circles.

The relations among angles and edge lengths are governed by cosine laws. Meshes with different background geometries require the corresponding cosine laws.

Discrete Riemannian Metric In the discrete setting, the edge lengths on a mesh Σ simply define the *discrete Riemannian metric* on Σ,

$$l : E \to \mathbb{R}^+,$$

such that for a face f_{ijk} the edge lengths satisfy the triangle inequality,

$$l_{ij} + l_{jk} > l_{ki}.$$

The discrete metric determines the angles. Suppose we have a triangle f_{ijk} with edge lengths $\{l_{ij}, l_{jk}, l_{ki}\}$, and the angles against the corresponding edges are $\{\theta_k, \theta_i, \theta_j\}$. The cosine laws with respect to the background geometries are

$$
\begin{aligned}
l_{ij}^2 &= l_{jk}^2 + l_{ki}^2 - 2l_{jk}l_{ki}\cos\theta_k, & \mathbb{E}^2 \\
\cosh l_{ij} &= \cosh l_{jk}\cosh l_{ki} - \sinh l_{jk}\sinh l_{ki}\cos\theta_k, & \mathbb{H}^2 \\
\cos l_{ij} &= \cos l_{jk}\cos l_{ki} + \sin l_{jk}\sin l_{ki}\cos\theta_k. & \mathbb{S}^2
\end{aligned}
\tag{12}
$$

Discrete Gaussian Curvature The discrete Gauss curvature is defined as the angle deficit on a mesh,

$$
K_i =
\begin{cases}
2\pi - \sum_{f_{ijk}\in F} \theta_i^{jk}, & \text{interior vertex} \\
\pi - \sum_{f_{ijk}\in F} \theta_i^{jk}, & \text{boundary vertex}
\end{cases}
\tag{13}
$$

where θ_i^{jk} represents the corner angle attached to vertex v_i in the face f_{ijk}.

Discrete Gauss-Bonnet Theorem In the discrete setting, the Gauss-Bonnet theorem (Eqn. 4) still holds on meshes with the discrete Gaussian curvatures, as follows.

$$\sum_{v_i\in V} K_i + \lambda \sum_{f_i\in F} A_i = 2\pi\chi(M),$$

where A_i denotes the area of face f_i, and λ represents the constant curvature for the canonical geometry; $+1$ for sphere, 0 for plane, and -1 for hyperbolic space.
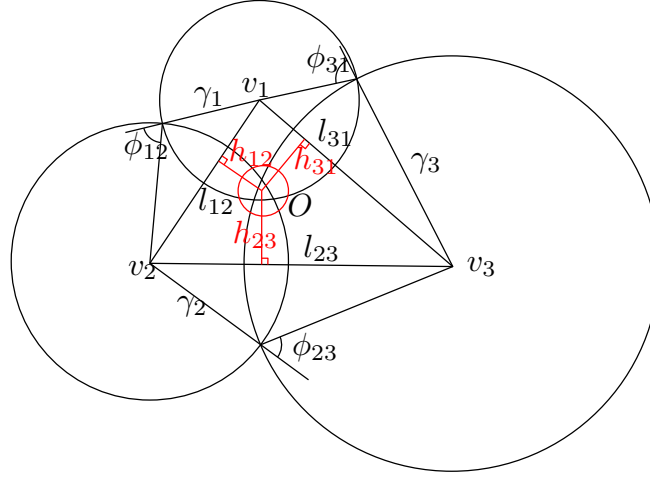
Fig. 9. Circle Packing Metric: Circle packing metric for a triangle. The center circle is the dual circle, which is orthogonal to all the other three circles

Discrete Conformal Deformation

In order to approximate conformal deformation of metrics, the circle packing metric is introduced [27, 40]. Let us denote Γ as a function which assigns a radius γ_i to each vertex v_i.

$$\Gamma : V \to \mathbb{R}^+$$

Similarly, let a *weight* on the mesh be a function,

$$\Phi : E \to [0, \frac{\pi}{2}].$$

on each edge e_{ij} by assigning a positive number $\Phi(e_{ij})$. The pair of vertex radius and edge weight functions on a mesh Σ, (Γ, Φ), is called a *circle packing metric* of Σ. Figure 9 illustrates the circle packing metrics. Each vertex v_i has a circle whose radius is r_i. On each edge e_{ij}, an intersection angle ϕ_{ij} is defined by two circles of v_i and v_j, which are intersected with or tangent to each other. Two circle packing metrics (Γ_1, Φ_1) and (Γ_2, Φ_2) on a same mesh are *conformal equivalent*, if $\Phi_1 \equiv \Phi_2$. Therefore, a conformal deformation of a circle packing metric only modifies the vertex radii.

For a given mesh, its circle packing metric and the edge lengths on the mesh can be converted to each other by using cosine laws. Here, the choice of the cosine laws is dependent on the background geometry of the mesh,

$$
\begin{aligned}
l_{ij}^2 &= \gamma_i^2 + \gamma_j^2 + 2\gamma_i\gamma_j \cos\phi_{ij}, & \mathbb{E}^2 \\
\cosh l_{ij} &= \cosh\gamma_i \cosh\gamma_j + \sinh\gamma_i \sinh\gamma_j \cos\phi_{ij}, & \mathbb{H}^2 \\
\cos l_{ij} &= \cos\gamma_i \cos\gamma_j - \sin\gamma_i \sin\gamma_j \cos\phi_{ij}. & \mathbb{S}^2
\end{aligned}
\tag{14}
$$

5.1   Theories on Discrete Ricci Flow

The connections between the circle packing metric and the discrete Gaussian curvature can be obtained from Eqn. 14 and 13. Now, we are ready to explain the discrete Ricci flow.

Let u_i to be

$$u_i = \begin{cases} \log \gamma_i & \mathbb{E}^2 \\ \log \tanh \frac{\gamma_i}{2} & \mathbb{H}^2 \\ \log \tan \frac{\gamma_i}{2} & \mathbb{S}^2 \end{cases} \qquad (15)$$

for each vertex. Then, the discrete Ricci flow is defined as follows.

$$\frac{du_i(t)}{dt} = (\bar{K}_i - K_i) \qquad (16)$$

Recall that, in continuous cases, Riemannian metrics determine the Gaussian curvature, and continuous Ricci flow is the conformal deformation of the Riemannian metric such that the deformation is proportional to the Gaussian curvature. Similarly, in discrete case, the circle packing metric determines the discrete Gaussian curvature (Eqn. 14, 13, and 12), and the discrete Ricci flow conformally deforms the circle packing metrics with respect to the Gaussian curvatures (Eqn. 15 and 16).

Discrete Ricci flow can be formulated in the variational setting, namely, it is a negative gradient flow of some special energy form. Let Σ be a spherical (Euclidean or hyperbolic) triangle mesh, then for arbitrary two vertices v_i, v_j, the following symmetric relation holds

$$\frac{\partial K_i}{\partial u_j} = \frac{\partial K_j}{\partial u_i}.$$

Let $\omega = \sum_{i=1}^{n} K_i du_i$ be a differential one-form [41]. The symmetric relation guarantees the one-form is closed (curl free)

$$d\omega = \sum_{i,j} (\frac{\partial K_i}{\partial u_j} - \frac{\partial K_j}{\partial u_i}) du_i \wedge du_j = 0.$$

Furthermore, the vertex radii **u** domain is simply connected, by Stokes theorem, the following integration is path independent,

$$f(\mathbf{u}) = \int_{\mathbf{u_0}}^{\mathbf{u}} \sum_{i=1}^{n} (\bar{K}_i - K_i) du_i, \qquad (17)$$

where $\mathbf{u_0}$ is an arbitrary initial metric. Therefore, the above integration is well defined, and called the *Ricci energy*. The discrete Ricci flow is the negative gradient flow of the discrete Ricci energy. The discrete metric which induces $\bar{k}$ is the minimizer of the energy.

Computing desired metric with prescribed curvature $\bar{K}$ is equivalent to minimizing the discrete Ricci energy. For Euclidean (or hyperbolic) case, the discrete Ricci energy is strictly convex (namely, its Hessian is positive definite). The global minimum uniquely exists, corresponding to the metric $\bar{\mathbf{u}}$, which induces $\bar{\mathbf{k}}$. The discrete Ricci flow
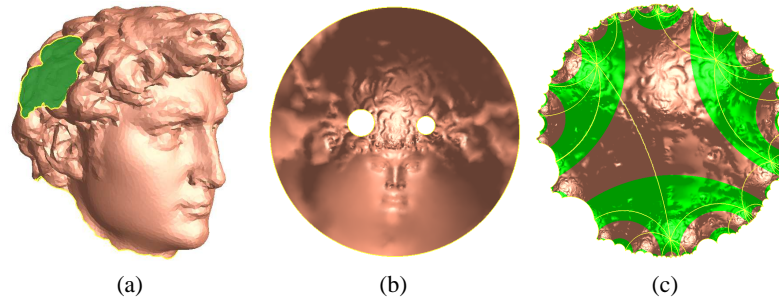
(a)   (b)   (c)

Fig. 10. The David head surface is a two-holed disk, shown in (a). It is parameterized as a planar multi-holed annulus, shown in (b). It can also be parameterized in the Poincaré disk, such that all boundaries are mapped to geodesics, shown in (c).

converges to this global minimum [11]. The Euclidean Ricci energy is strictly convex on the space of normalized metric $\sum u_i = 0$. The hyperbolic Ricci energy is strictly convex. The Spherical Ricci energy is not strictly convex, the desired metric $\bar{\mathbf{u}}$ is still a critical point of the energy and can be reached by the Ricci flow (gradient descent) method.

6   Applications

Discrete Ricci flow is a powerful tool for computing the desired metrics with the prescribed Gaussian curvatures on general surfaces. Many applications in graphics and geometric modeling can be formulated as the problem of finding specific metrics for prescribed curvatures. The followings are some applications directly related with discrete Ricci flow.

6.1   Global Conformal Parameterization

Surface parameterization in conventional computer graphics refers to the process of mapping a surface to a canonical domain. Ricci flow is an effective approach for fully automatic, seam-free, and singularity-free parameterization of arbitrarily complicated surfaces.

For closed surfaces, we compute their uniformization metric and embed their universal covering spaces onto the three canonical spaces, as described in the uniformization theorem. Fig.1 illustrates the global parameterizations of surfaces with different topologies with their uniformization metrics respectively.

For surfaces with boundaries, there are two general ways. In the first way, we map the interior of the surface to planar domains, and the boundaries to circles. In the second way, the surface is embedded onto the canonical spaces with its uniformization metric, such that all the boundaries are mapped to geodesics. Fig. 10 shows one example, where a genus zero surface with three boundaries are parameterized in both ways.

In general case, both the positions and curvatures of singularities can be arbitrarily chosen, as long as the Gauss-Bonnet condition and the connectivity constraints hold, the

metric can be obtained using Ricci flow method. The flexibility of assigning singularities greatly improves the quality of conformal parameterizations. Fig.11 demonstrates the parameterizations of scanned surfaces using this method.
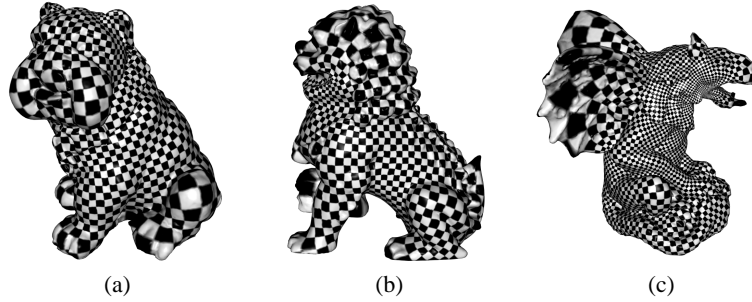

(a)   (b)   (c)

Fig. 11. Parameterizations of scanned surfaces using discrete Ricci flow.

6.2   Surface Matching

Surface matching is a fundamental problem in geometric processing. The main framework of surface matching using Ricci flow can be formulated in the following commutative diagram,

$$
\begin{array}{ccc}
S_1 & \xrightarrow{\ \phi\ } & S_2 \\
\tau_1 \downarrow & & \downarrow \tau_2 \\
D_1 & \xrightarrow{\ \bar{\phi}\ } & D_2
\end{array}
\tag{18}
$$

S_1, S_2 are two given surfaces, $\phi : S_1 \rightarrow S_2$ is the desired matching. We use Ricci flow to compute $\tau_i : S_i \rightarrow D_i$ which maps S_i conformally onto the canonical domain D_i. D_1 and D_2 can also be surfaces other than simple planar domains. The topology and the curvature of D_1 and D_2 incorporate the major feature information of the original surfaces S_1 and S_2. The we construct a harmonic map $\bar{\phi} : D_1 \rightarrow D_2$. If there are certain feature constraints, they can be incorporated in $\bar{\phi}$. The final map ϕ is induced by $\phi = \tau_2^{-1} \circ \bar{\phi} \circ \tau_1$. Fig.12 shows one example of surface matching between two genus one surfaces with three boundaries. Both of them are mapped onto the plane with circular boundaries, D_1 and D_2 chosen to be their fundamental domains. The harmonic map is calculated between the two fundamental domains. The mapping result is illustrated by consistent texture mapping.

6.3   Computing General Geometric Structures

Suppose S is a surface, $\mathscr{A} = \{(U_\alpha, \phi_\alpha)\}$ is an atlas of S. If all the local coordinates $\phi_\alpha(U_\alpha)$ is in a special space X, and all the chart transition functions $\phi_{\alpha\beta}$ to a special
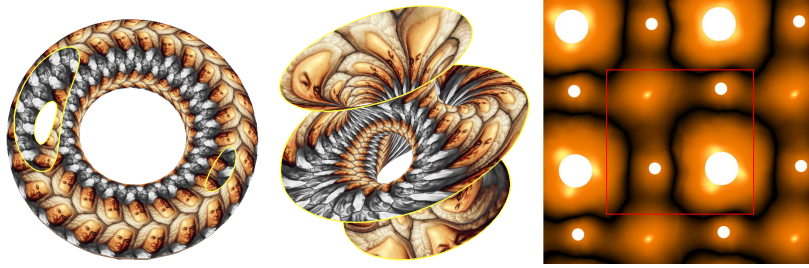
Fig. 12. Two genus one surfaces with 3 bounaries are conformally parameterized onto the plane, such that their boundaries are mapped to circles. Then a map is constructed between their planar images, which induces a matching between them. The matching is visualized by the consistent texture mapping.

group G, which is a subgroup of the automorphism group of X, then $\mathscr{A}$ is called a (X, G) structure of S.

All genus zero closed surfaces can be conformally mapped onto the sphere, namely, they admit spherical structures, (see Fig.1)

Suppose X is the two dimensional affine space $\mathbb{A}^2$, and G is the affine transformation group, then the atlas is called an *Affine Structure* of S. Affine structure plays fundamental role in manifold splines. For closed surfaces, only genus one surfaces have affine structures. All surfaces with boundaries admit affine structures.

If X is the hyperbolic space $\mathbb{H}^2$, and G is the hyperbolic rigid motion (Möbius transformation), the the atlas is called a *hyperbolic space*. Surfaces with negative Euler number admit hyperbolic structures. Fig. 13 demonstrates the hyperbolic structures of genus two surfaces.

All surfaces have real projective structures, where the coordinates are in the real projective space $\mathbb{RP}^2$, and the chart transition functions are real projective transformations. For high genus surfaces, the real projective structure can be constructed by using hyperbolic Ricci flow to compute the hyperbolic uniformization metric, then isometrically embedding the universal covering space onto the Klein hyperbolic space model.

6.4 Manifold Splines

Conventional splines are defined on planar domains. However, it is natural to define splines directly on surfaces with general topologies. The concept of manifold splines was first introduced in [9], where the splines are defined on manifold domains and the evaluations of the splines are independent of the choice of the local charts.

The significant advantage of the manifold spline is that it is globally defined, but locally on each chart, a common planar spline. As it has been proved that defining splines over arbitrary manifolds is equivalent to the existence of an affine atlas of the underlying manifold. The affine atlas can be constructed by holomorphic 1-form method [19], as described in [9]. The positions of zero points can not be specified, which are solely determined by the conformal structure and the holomorphic 1-form. The affine struc-
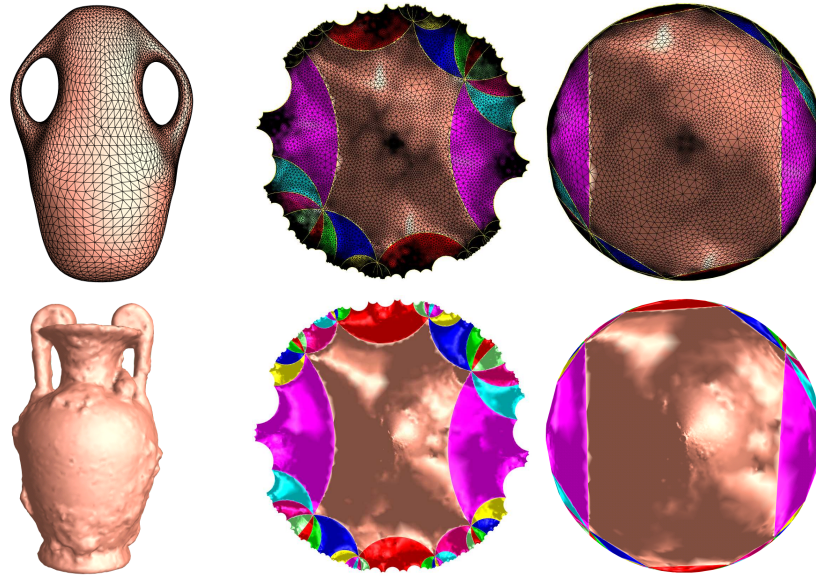
Fig. 13. Hyperbolic structure and real projective structure of genus two surfaces.

ture can also be constructed using Ricci flow, while the singularities can be arbitrarily chosen.

Fig.14 shows this problem with genus three sculpture model, which has to carry four zero points when constructing manifold spline. Even for genus-1 surfaces with boundaries, since differential forms method does not work directly on open surfaces, the construction of manifold splines is still not able to avoid singular points after double covering which converts open surfaces to closed ones.

With Euclidean Ricci flow, all the curvatures of a given domain manifold can be put on one vertex or boundaries, such that the special metric of the domain manifold is flat everywhere except at one singular point. Then, the metric induces an affine atlas covering the whole manifold except the singular point, and manifold spline is constructed over this affine atlas. Fig.15 shows the an example of a genus-3 model with only one singular point when constructing manifold spline using Euclidean Ricci flow.

7   Conclusion and Future Works

This work introduces a powerful tool: discrete surface Ricci flow, borrowed from continuous Ricci flow from modern geometry for computing Riemannian metrics with prescribed Gaussian curvatures on discrete surfaces. For practical use, the concepts of Riemannian metric and Gaussian curvature are translated to discrete setting; the discrete analogy of Ricci flow is designed; the existence and uniqueness of the solution of the discrete Ricci flow is verified; and efficient numerical algorithms to compute Riemannian metrics with prescribed Gaussian curvatures using discrete Ricci flow for generally topological surfaces are presented in details.
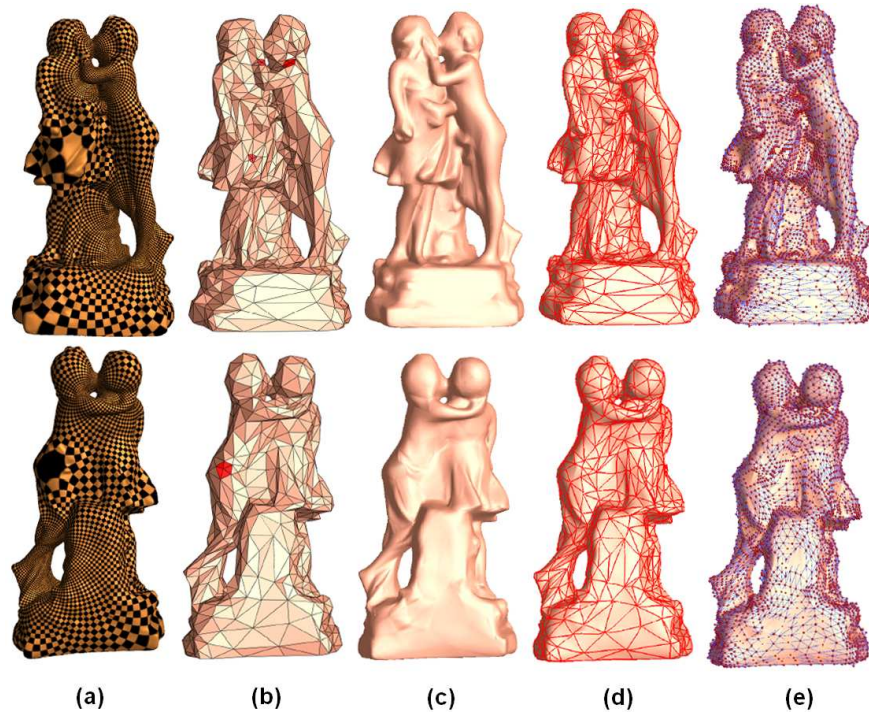
Fig. 14. Manifold Spline of Sculpture Model Constructed Using Differential Forms With 4 Singular Points (see more details in [9]): (a) Holomorphic 1-form which induces the affine atlas $\mathbb{A}$; (b) Parametric domain manifold M with singular points marked; (c) Polynomial spline F defined on the manifold M in (a); (d) The red curves on spline F correspond to the edges in the domain manifold M; (e) Spline F covered by control net C.

Several applications in graphics and geometric modeling, such as surface parameterization, surface matching, manifold splines, and construction of geometric structures on general surfaces are demonstrated.

The discrete theory and computational methodologies for Teichmüller space theory are widely open. The rigorous theoretic results about the convergence to the smooth conformal structure and the approximation accuracy of discrete Ricci flow have not been established. In the future, we will continue our exploration along these directions.
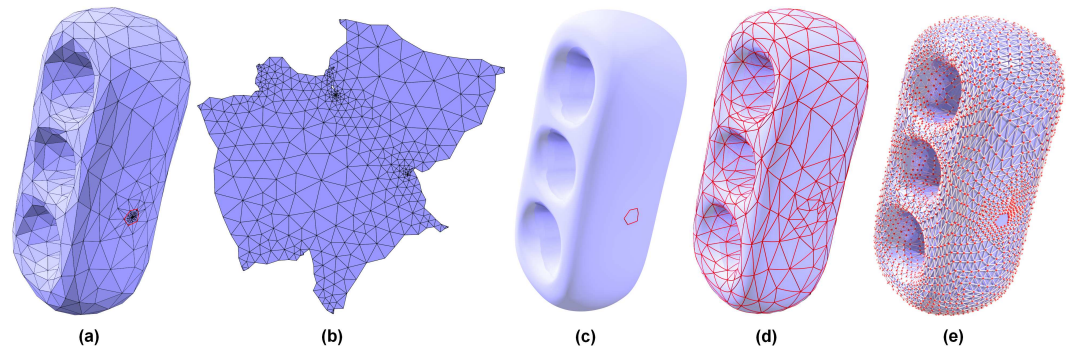
8   Acknowledgement

Fig. 15. Manifold Spline of Genus-3 Model Constructed Using discrete Euclidean Ricci Flow With Only One Singular Point (see more details in [36]): (a) Domain manifold (b) Central chart (c) Manifold triangular B-spline (d) Manifold triangular B-spline (e) Control points.

References

1. G. Perelman, "The entropy formula for the ricci flow and its geometric applications," Tech. Rep. arXiv.org, November 11 2002.
2. G. Perelman, "Ricci flow with surgery on three-manifolds," Tech. Rep. arXiv.org, March 10 2003.
3. G. Perelman, "Finite extinction time for the solutions to the ricci flow on certain three-manifolds," Tech. Rep. arXiv.org, July 17 2003.
4. R. S. Hamilton, "Three manifolds with positive ricci curvature," *Journal of Differential Geometry.*, vol. 17, pp. 255–306, 1982.
5. B. Lévy, S. Petitjean, N. Ray, and J. Maillot, "Least squares conformal maps for automatic texture atlas generation," *SIGGRAPH 2002*, pp. 362–371, 2002.
6. M. Botsch and L. Kobbelt, "An interactive framework for real-time freeform modeling," *ACM Transactions on Graphics (SIGGRAPH 2004)*, vol. 23, no. 3, pp. 630–634, 2004.
7. P. Alliez, M. Meyer, and M. Desbrun, "Interactive geometry remeshing," *SIGGRAPH 2002*, pp. 347–354, 2002.
8. C. Grimm and D. Zorin, *Surface Modeling and Parameterization with Manifolds*. SIGGRAPH 2006 course notes, 2006.
9. X. Gu, Y. He, and H. Qin, "Manifold splines," *Graphical Models*, vol. 68, no. 3, pp. 237–254, 2006.
10. X. Gu, Y. Wang, T. F. Chan, P. M. Thompson, and S.-T. Yau, "Genus zero surface conformal mapping and its application to brain surface mapping," *IEEE Transactions on Medical Imaging*, vol. 23, no. 8, pp. 949–958, 2004.
11. B. Chow and F. Luo, "Combinatorial ricci flows on surfaces," *Journal Differential Geometry*, vol. 63, no. 1, pp. 97–129, 2003.
12. M. S. Floater and K. Hormann, "Surface parameterization: a tutorial and survey," in *Advances in Multiresolution for Geometric Modelling*, pp. 157–186, Springer, 2005.
13. V. Kraevoy and A. Sheffer, "Cross-parameterization and compatible remeshing of 3d models," *ACM Transactions on Graphics*, vol. 23, no. 3, pp. 861–869, 2004.
14. M. Desbrun, M. Meyer, and P. Alliez, "Intrinsic parameterizations of surface meshes," *Computer Graphics Forum (Proc. Eurographics 2002)*, vol. 21, no. 3, pp. 209–218, 2002.

15. U. Pinkall and K. Polthier, "Computing discrete minimal surfaces and their conjugates," *Experimental Mathematics*, vol. 2, no. 1, pp. 15–36, 1993.

16. M. S. Floater, "Mean value coordinates," *Computer Aided Geometric Design*, vol. 20, no. 1, pp. 19–27, 2003.

17. R. Zayer, C. Rössl, and H.-P. Seidel, "Setting the boundary free: A composite approach to surface parameterization," in *Eurgraphics Symposium on Geometry Processing* (M. D. Pottmann and H., eds.), pp. 91–100, 2005.

18. C. Gotsman, X. Gu, and A. Sheffer, "Fundamentals of spherical parameterization for 3d meshes," *ACM Transactions on Graphics*, vol. 22, no. 3, pp. 358–363, 2003.

19. X. Gu and S.-T. Yau, "Global conformal parameterization," in *Symposium on Geometry Processing*, pp. 127–137, 2003.

20. C. Mercat, "Discrete riemann surfaces and the ising model," *Communications in Mathematical Physics*, vol. 218, no. 1, pp. 177–216, 2004.

21. A. N. Hirani, *Discrete exterior calculus*. PhD thesis, California Institute of Technology, 2003.

22. M. Jin, Y. Wang, S.-T. Yau, and X. Gu, "Optimal global conformal surface parameterization," in *IEEE Visualization 2004*, pp. 267–274, 2004.

23. S. J. Gortler, C. Gotsman, and D. Thurston, "Discrete one-forms on meshes and applications to 3D mesh parameterization," *Computer Aided Geometric Design*, vol. 23, no. 2, pp. 83–112, 2005.

24. Y. Tong, P. Alliez, D. Cohen-Steiner, and M. Desbrun, "Designing quadrangulations with discrete harmonic forms," in *Symposium on Geometry Processing*, pp. 201–210, 2006.

25. A. Sheffer and E. de Sturler, "Parameterization of faced surfaces for meshing using angle based flattening," *Engineering with Computers*, vol. 17, no. 3, pp. 326–337, 2001.

26. A. Sheffer, B. Lévy, M. Mogilnitsky, and A. Bogomyakov, "ABF++: Fast and robust angle based flattening," *ACM Transactions on Graphics*, vol. 24, no. 2, pp. 311–330, 2005.

27. W. P. Thurston, *Geometry and Topology of Three-Manifolds*. Princeton lecture notes, 1976.

28. B. Rodin and D. Sullivan, "The convergence of circle packings to the riemann mapping," *Journal Differential Geometry*, vol. 26, no. 2, pp. 349–360, 1987.

29. C. Collins and K. Stephenson, "A circle packing algorithm," *Computational Geometry: Theory and Applications*, vol. 25, pp. 233–256, 2003.

30. Y. C. de Verdiére, "Un principe variationnel pour les empilements de cercles," *Journal Differential Geometry*, vol. 104, no. 3, pp. 655–669, 1991.

31. A. I. Bobenko and B. A. Springborn, "Variational principles for circle patterns and koebe's theorem," *Transactions of the American Mathematical Society*, vol. 356, pp. 659–689, 2004.

32. L. Kharevych, B. Springborn, and P. Schröder, "Discrete conformal mappings via circle patterns," *ACM Transactions on Graphics*, vol. 25, no. 2, pp. 412–438, 2006.

33. B. Springborn, "Variational principles for circle patterns," 2003.

34. R. S. Hamilton, "The ricci flow on surfaces," *Mathematics and general relativity*, vol. 71, pp. 237–262, 1988.

35. M. Jin, F. Luo, and X. Gu, "Computing surface hyperbolic structure and real projective structure," in *ACM Symposium on Solid and Physics Modeling*, pp. 105–116, 2006.

36. X. Gu, Y. He, M. Jin, F. Luo, H. Qin, and S.-T. Yau, "Manifold splines with single extraordinary point," in *ACM Symposium on Solid and Physics Modeling*, p. to appear, 2007.

37. H. W. Guggenheimer, *Differential Geometry*. Dover Publications, 1977.

38. H. M. Farkas and I. Kra, *Riemann Surfaces*. Springer, 2004.

39. B. Chow, "The ricci flow on the 2-sphere," *J. Differential Geom.*, vol. 33, no. 2, pp. 325–334, 1991.

40. K. Stephenson, *Introduction To Circle Packing*. Cambridge University Press, 2005.

41. S. H. Weitraub, *Differential Forms: A Complement to Vector Calculus*. Academic Press, 2007.